The demand response potential in copper production

Journal of Cleaner Production 362 (2022) 132221

Contents lists available at ScienceDirect

Journal of Cleaner Production

journal homepage: www.elsevier.com/locate/jclepro

The demand response potential in copper production

Fritz T.C. Röben [a,b], Diran Liu [a], Markus A. Reuter [c], Manuel Dahmen [a], André Bardow [d,a,e,f,*]

[a] Institute of Energy and Climate Research - Energy Systems Engineering (IEK-10), Forschungszentrum Jülich GmbH, 52425, Jülich, Germany
[b] RWTH Aachen University, 52062 Aachen, Germany
[c] SMS group GmbH, 40237 Düsseldorf, Germany
[d] JARA-ENERGY, 52425 Jülich, Germany
[e] Institute of Technical Thermodynamics, RWTH Aachen University, 52062 Aachen, Germany
[f] Energy & Process Systems Engineering, ETH Zürich, 8092 Zürich, Switzerland

ARTICLE INFO

Handling Editor: Kathleen Aviso

Keywords:
Demand side management (DSM)
Demand response
Resource-task network (RTN)
Scheduling optimization
Copper production

ABSTRACT

Demand response (DR) of large industrial electricity consumers is a promising option to balance the fluctuating supply by renewable energies in the electricity grid. Renewable energy technologies themselves depend on copper as a key material. At the same time, the production of copper is a power-intensive process but its DR potential has not yet been quantified in detail via process scheduling.

Here, we analyze the DR potential of copper production by optimally scheduling the batch and continuous tasks of a representative copper process. To determine the optimal schedule, we formulate a mixed-integer linear program (MILP) based on the resource-task network (RTN) formulation approach. We first optimize the production volume to define a reference case and then minimize the electricity costs under time-varying electricity prices while retaining the production target. A sensitivity analysis evaluates the impact of task capacities on the production volume and DR potential.

The results indicate a significant DR potential, as optimal scheduling can reduce the annual electricity costs by up to 14.2% while still producing the maximum copper output as the reference process schedule. The power-intensive electrolytic refining shows the largest potential for reducing costs. Offgas handling, air separation, and air compression further show significant cost reduction potentials. These tasks must process large material streams that are directly connected to operating the smelting and refining tasks. Our model shows the potential of considering these interlinked tasks in one scheduling model that focuses on DR.

The results suggest that DR scheduling in copper production has a significant economic potential without compromising production goals. Further, the DR scheduling shifts large amounts of electricity demand by responding to fluctuating electricity prices, which enables flexibility of the demand side and can thus support the integration of renewable energy into the electric grid.

1. Introduction

The growing share of renewable energy in the electricity grid requires the balancing of fluctuations in the electricity supply. A promising option is demand side management (DSM) of industrial processes (Paulus and Borggrefe, 2011). DSM adjusts the energy demands of consumers, which in industry typically includes adjusting the production processes and energy supply (Zhang and Grossmann, 2016). Potentially, DSM benefits both grid operators and consumers by stabilizing the electricity grid and reducing electricity costs (Zhang and Grossmann, 2016). One category of DSM is demand response (DR) which focuses on adjusting a consumer's load profile in response to economic incentives. Economic incentives typically include time-varying electricity prices for the consumer, such as hourly electricity prices on the day-ahead market. Thus, DR offers potential an economic potential for industry while enabling flexibility for the grid (Heffron et al., 2020).

The DR potential for industrial electricity demand in Europe is expected to be immense and could contribute significantly to a cost-effective transition to a low-carbon energy system (Papadaskalopoulos et al., 2018): Economically, DR is expected to reduce costs by billions of Euro per year through avoiding investments in additional capacities for generation, transmission, and distribution as well as operational costs. Environmentally, flexible process operations due to DR can increase the utilization of renewable energy generation by shifting the demand to times of high energy availability. For example, Finn and Fitzpatrick (2014) show that the cost-optimal load shifting of an industrial

* Correspondence to: Energy & Process Systems Engineering, ETH Zürich, CLA F19.1 Tannenstrasse 3, 8092 Zürich, Switzerland.
E-mail address: abardow@ethz.ch (A. Bardow).

https://doi.org/10.1016/j.jclepro.2022.132221
Received 18 November 2021; Received in revised form 21 April 2022; Accepted 11 May 2022
Available online 19 May 2022

consumer can increase wind power consumption in Ireland. Further, DR typically offers higher efficiencies than many other balancing options that use energy conversion technologies, e.g., power-to-gas (Heffron et al., 2020).

A significant interest in DR of energy-intensive industries can be seen in the many recent studies on, e.g., air separation, aluminium, or cement production, as reviewed by Zhang and Grossmann (2016). These studies indicate a high economic potential for the respective industries to reduce operating costs by optimally scheduling their production with DR in mind. Considering energy demands in scheduling is a logical step, as the timing of consumption can significantly affect energy bills, particularly given the growing share of renewable energy supply (Merkert et al., 2015). However, the DR potential in copper production has only been analyzed based on strongly-simplifying assumptions until now, and only with regard to the most power-intensive sub-processes, e.g., in Gils (2014) or Röben et al. (2019). Quantification of the DR potential in copper production at the process level by optimally scheduling the production is missing so far. However, a detailed scheduling is important to capture the process structure and dependencies between the many materials and tasks in the production.

Assessing the DR potential of copper production is important also due to the expected substantial increase in future copper demand. The global demand is expected to triple from 2010 to 2050 (Elshkaki et al., 2016), strongly driven by socio-economic development worldwide (Elshkaki et al., 2016; Deetman et al., 2018; Henckens and Worrell, 2020). As copper is a key material for low-carbon technologies like electric vehicles and renewable energy systems (Deetman et al., 2018; Kuipers et al., 2018; IEA, 2021), the global shift towards high shares of renewable energy sources increases the global copper demand (Schipper et al., 2018). The International Energy Agency (IEA) expects that the large-scale implementation of low-carbon technologies will account for up to 40% of the global copper demand in 2040, also due to their higher copper demand compared to fossil-fueled technologies (IEA, 2021). At the same time cooper production itself is an energy-intensive process consuming large amounts of fossil fuels and electricity that must be integrated into an increasingly renewable energy system. Thus, the flexible adjustment of the power demand by DR becomes particularly relevant and is an important step towards integrating renewable energy into copper production (Moreno-Leiva et al., 2019).

Available scheduling models of copper production mainly focus on maximizing the process throughput, e.g., Harjunkoski et al. (2006), Suominen et al. (2016), Navarra et al. (2017). Harjunkoski et al. (2006) present such a scheduling model that considers the production tasks of flash smelting, converting, fire-refining, and casting, while further including the cranes that transport materials in the plant. The model includes processing times that vary due to changes in the input materials with a scheduling horizon of 36 h. Similarly, the model of Pradenas et al. (2006) optimizes the throughput of a copper production plant in Chile while paying special attention to compliance with tightened environmental regulations such as offgas release. A later model focuses on minimizing the makespan of the refining and casting operations in copper production with a heuristic approach (Pradenas et al., 2011). Suominen et al. (2016) present a nonlinear scheduling optimization problem that considers the flash smelting and converting tasks to optimize key figures such as flash smelting production rate and deviation from a predefined matte grade. Navarra et al. (2017) present a discrete-event simulation (DES) framework that adapts operation to comply with environmental constraints, which is necessary due to changing weather situations. The uncertainty of the weather forecast is analyzed, and the operation is simulated for a wide range of scenarios. In another contribution, Navarra (2016) use a greedy heuristic in a DES to schedule the converter operation. Recently, Korpi et al. (2019) presented a two-level structure to optimize copper production and enable model-based control of the processes. On the upper level, a mixed-integer linear program (MILP) optimally schedules the operation of the processes. On the lower level, detailed process models enable control of operating parameters and states. These detailed sub-models can also be used on their own and are already included in industrial software (Korpi et al., 2019). However, the mathematical formulation of the MILP scheduling model is not disclosed.

A broader planning model is presented by Siemon et al. (2020), which targets the optimal economic production of a copper plant, including the blending of copper ore concentrates with different compositions from several mines. The recent model extension in Siemon et al. (2021) further includes raw material purchasing and shipment decisions in multi-plant networks. In result, these planning models account for long time horizons of several months, e.g., 90 days in Siemon et al. (2021) and the chosen resolution of the time horizon of one day is too coarse for considering DR. While many technical and economic constraints are implemented in these planning models, the batch-wise operation structure is not resolved and the sub-processes are represented with steady-state operating points.

Thus, models to optimize the operation of copper production exist but focus primarily on optimizing the plant throughput. As the existing scheduling models do not consider electricity demands and planning models do not include the operational detail of the batch structure and necessary time resolution, a new scheduling model is required that is suitable to determine the DR potential in copper production.

In this work, we formulate a new scheduling model which represents the process structure on a task-specific level, including all tasks that have significant electricity demands, and considers the electricity costs under time-varying electricity prices. We first determine a reference schedule by maximizing the production volume neglecting the electricity costs and then determine the cost-optimal schedule by minimizing the electricity costs while keeping the production target. We evaluate the economic benefit and analyze the amount of shifted electricity demand over several schedules in the year and assess the contribution of the different tasks. Since the capacity of a task has a substantial influence on the available flexibility, we perform a sensitivity analysis of the most important tasks with regard to the DR potential and determine the respective impact on the production volume and the electricity costs.

The remainder of the paper is structured as follows: Section 2 gives a brief overview of the copper production process and the considered tasks. Section 3 presents the optimization problem formulation and the parameters used in our model. Section 4 first analyzes the influence of the scheduling horizon on the production volume, then presents the results for the different schedules throughout the year, further shows the sensitivity analysis of the critical tasks, and finally discusses the implications of this work. Finally, conclusions are drawn in Section 5.

2. Copper production

In this section, we briefly describe a representative copper production process (Fig. 1) which produces high-purity copper cathodes from copper concentrates through smelting and refining. The process description is based on Schlesinger et al. (2011).

The copper concentrate used in the flash furnace has typically been concentrated up to 30 wt-% copper at the mining site. In the flash furnace, the concentrate is continuously blown into the furnace in an oxygen-enriched blast of 50–70 vol-% O_2. In the blast, iron and sulfur in the concentrate oxidize, which leads to a large heat release that melts the solids. Thus, a large amount of energy is introduced into the process by the ore. The molten material gathers in the furnace bath, where it separates into two layers. The heavier copper-rich matte (50–70 wt-% Cu) gathers at the bottom and the lighter slag, containing mainly iron oxides, gathers at the top. When enough matte has been accumulated, a part of the matted is tapped and sent to the converters. The slag in the flash furnace is sent to the slag-cleaning furnace to recover matte droplets that have not separated quickly enough. The residence time in the slag-cleaning furnace lasts around five hours,

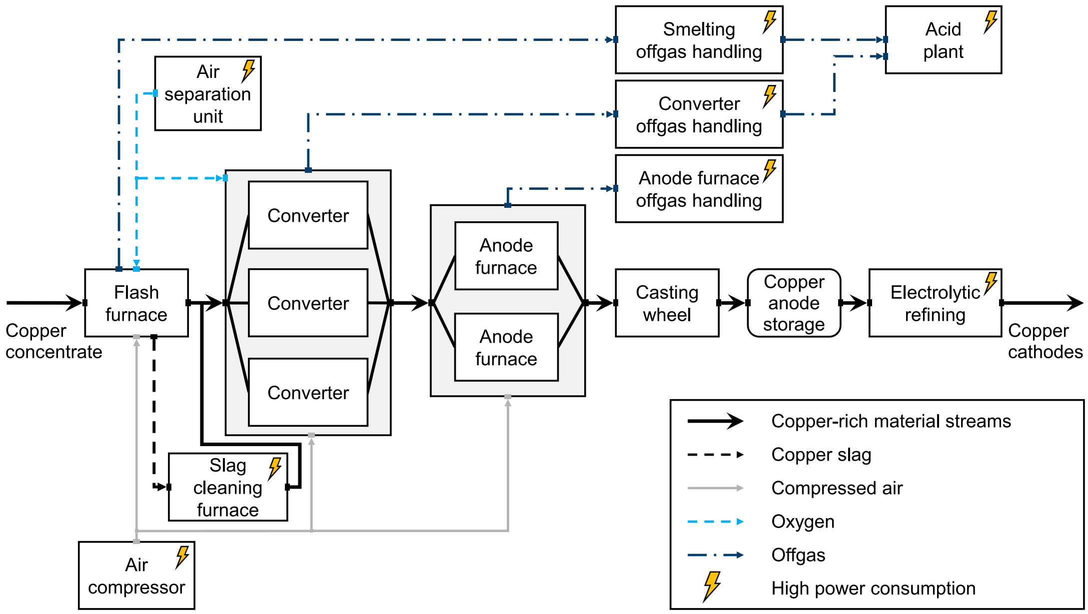

Fig. 1. Simplified flowsheet of the representative copper production process. The flowsheet shows the material stream concentrating the copper (solid black arrows) as well as other material streams associated with tasks that require significant power. The lightning symbol indicates tasks with high power consumption.

during which the slag is kept hot by electric resistive heating. The recovered matte is intermittently tapped and added to the converters along with the matte from flash smelting. In the converters, iron and sulfur in the matte are further oxidized by blowing compressed air through the matte. The oxidation also heats up the converter. Plants often use oxygen-enriched air of around 22–28 vol-% O_2, with 23 vol-% O_2 being used in our process. The iron oxides form a slag which is removed, and the sulfur forms sulfur dioxide, which is collected by the offgas system. The converting takes place in batches lasting several hours. Thus, plants generally have two to five converters depending on their smelting capacity, with our production process having three converters. The final product of the converting is blister copper of 99 wt-% copper. A batch of blister copper is then sent to an anode furnace where the remaining dissolved sulfur and oxygen are removed by blowing first compressed air and then a reducing agent, e.g., natural gas, through the melt. This process is called fire-refining. The resulting molten copper with a purity of around 99.5 wt-% is then cast into solid copper anodes. The casting of one batch takes several hours due to the solidifying and cooling speed of the copper anodes on the casting wheel. Including casting, the total processing time of one batch is about 9 h, so plants usually have multiple anode furnaces feeding one casting wheel, i.e., two in our process. The final step is the electrorefining, which consists of electrolytically dissolving the copper anodes into an electrolyte and plating the copper from the electrolyte onto stainless steel cathodes. The final copper cathodes have a very high purity of over 99.99 wt-% copper.

Besides the electrolytic refining, other tasks require considerable amounts of electricity: As the flash furnace and converters require large amounts of oxygen, an air separation unit has to be operated, which constitutes an energy-intensive process by itself. The flash furnace, converters, and anode furnaces require large quantities of compressed air, which necessitates the operation of air compressors. Further, environmental protection measures can account for up to 30% of the electricity consumption of a plant (Grave et al., 2014). For example, large quantities of offgases have to be handled and cleaned before release into the atmosphere. The large amounts of sulfur dioxide (SO_2) formed by the oxidation in the flash smelting and converting have to be removed from the offgas. Typically, the sulfur dioxide is captured as sulfuric acid (Schlesinger et al., 2011), which is a by-product produced in large quantities. Note that the high electricity consumption of environmental protection measures such as high-efficiency offgas handling and cleaning refers to a best-practice approach. The use of elaborate offgas-cleaning technologies can be influenced by the strictness of local environmental regulations. Thus, the respective electricity demand can vary between production sites based on the local emission restrictions. The process we consider in this paper applies best-practice technologies in terms of environmental protection, particularly in terms of SO_2 capture and storage, and thus we assume that all offgases are treated at all times.

While the shown representative process (Fig. 1) is based on a specific design, it applies the most commonly used technologies for copper smelting and converting, i.e., flash smelting and Peirce–Smith converting (Wang et al., 2019). Moreover, the subsequent fire-refining and electrolytic refining are applied to virtually all molten copper to produce high-purity cathode copper, which can be used for electrical applications (Schlesinger et al., 2011). Thus, the formulated model is based on the most common process structure and should be as representative as possible to analyze the potential for DR in copper production.

3. Scheduling model description

In this section, we present the structure of our model and the approach to determine the optimal schedule.

3.1. Resource-task network and copper scheduling model

We formulate a mixed-integer linear program (MILP) to optimize the plant operation. The scheduling decisions include the timing of tasks and their magnitude of operation.

The scheduling model is formulated as a discrete-time resource-task network (RTN) (Pantelides, 1994). Resources include all materials, utilities, and equipment in the process. Tasks include all operations that consume, produce, or transport resources. Due to the general formulation and uniform handling of resources, the RTN formalism can describe a wide range of scheduling problems and is easy to extend (Pantelides, 1994; Wassick and Ferrio, 2011; Castro et al., 2019). RTNs have been shown to handle problems of industrial relevance (Wassick and Ferrio, 2011; Harjunkoski et al., 2014) and can be an important tool for industrial DR (Castro et al., 2013).

Discrete-time refers to the structure of the scheduling time horizon that is mapped onto a fixed time grid with time periods of typically uniform length (Harjunkoski et al., 2014). The prior knowledge of the time points in the time grid is the main advantage of a discrete-time representation as it makes modeling events during the task operation particularly easy (Sundaramoorthy and Maravelias, 2011; Castro et al., 2013; Harjunkoski et al., 2014). In our study, these events are time-varying electricity prices and material interactions during the execution of a task, i.e., materials can be consumed/produced in different amounts in each operating time step of a task.

Although a few scheduling models for copper production exist in the literature, the analysis of the DR potential requires a specific scheduling model for several reasons: First, existing scheduling models are mainly developed to maximize production under specific constraints (Harjunkoski et al., 2006; Pradenas et al., 2011; Suominen et al., 2016), while electricity demands, time-varying electricity prices, and DR potential are not considered. Second, most existing models typically focus on a part of the process which is critical for the respective analysis, e.g., crane operations (Harjunkoski et al., 2006) or environmental regulations (Pradenas et al., 2006). As the electricity costs have not been assessed yet, models often do not include tasks which cause large parts of the electricity demand. So, while these models consider specific process details, they are not suitable to evaluate the DR potential. Third, existing scheduling models typically use a continuous-time structure, which allows for an exact representation of processing times but makes implementing time-dependent electricity prices and material demands particularly difficult (Sundaramoorthy and Maravelias, 2011; Harjunkoski et al., 2014). However, this time-dependent material demand needs to be taken into account to determine the time-dependent electricity demand and thus the DR potential.

In conclusion, it is necessary to formulate a scheduling model which includes the electricity costs in the objective function and covers tasks that are crucial for the copper production volume and the electricity demand. The model needs to implement time-dependent costs and material demands, and represents the structure of the batch operations. By formulating such a model, we can determine the DR potential of the process.

3.2. Problem description

In this section, the formal equations of the scheduling model are presented. The equations are presented according to the RTN formalism (Pantelides, 1994).

We consider two objectives: maximization of the production volume and minimization of the electricity cost. The first objective determines the achievable production volume of the process to define a reference for the demand response case which minimizes the electricity cost. The maximum production objective is written as

$$\max \quad \sum_{t \in \mathcal{T}} \xi_{\mathrm{erf},t}, \tag{1}$$

where $\xi_{\mathrm{erf},t}$ is the extent of operation of the electrolytic refining (erf) in time step t. As the electrolytic refining produces the final product cathode copper, the production volume is maximized.

The minimal electricity cost objective is written as

$$\min \quad \sum_{t \in \mathcal{T}} \Pi_{\mathrm{el},t} \, ep_t, \tag{2}$$

where $\Pi_{\mathrm{el},t}$ is the total electricity consumption in time period t, and ep_t are the hourly-varying electricity prices.

The constraints of the scheduling model are written as given by the RTN formalism (Pantelides, 1994). The excess resource balance determines the resource availability through the scheduling time horizon by considering the change of the resource amount in each time step based

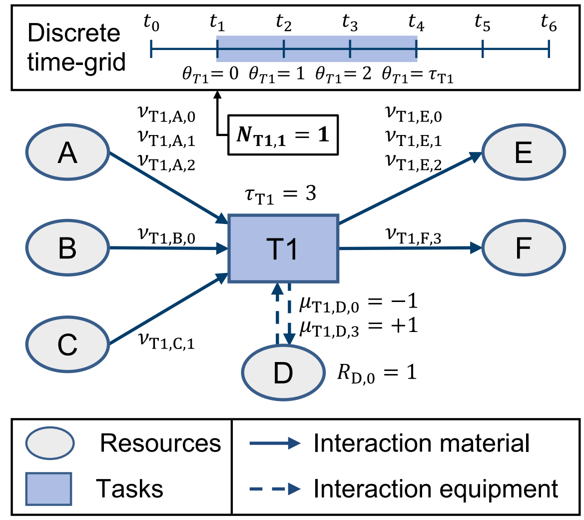

Fig. 2. RTN representation of an exemplary task T1. The global time grid is defined by t and the task-specific time that ranges from $\theta_i = 0$ to $\theta_i = \tau_i$ to define the time-dependent material interactions. The graphical representation of the RTN, which displays tasks as rectangles and resources as circles, is based on Pantelides (1994).

on the interactions with tasks and external material in-/outputs. The excess resource balance is written as

$$R_{r,t} = R_{r,t-1} + \sum_{i \in \mathcal{I}} \sum_{\theta_i = 0}^{\tau_i} \left(\mu_{i,r,\theta} \, N_{i,t-\theta} + \nu_{i,r,\theta} \, \xi_{i,t-\theta} \right) + \Pi_{r,t} \quad \forall r \in \mathcal{R}, \, t \in \mathcal{T}, \tag{3}$$

where $R_{r,t}$ represents the excess amount of resource r in time period t, with $\mathcal{R}$ as the set of all resources and $\mathcal{T}$ as the set of all time periods. $R_{r,t-1}$ is the amount of resource carried over from the previous time period. To account for the consumption and production of a resource, all tasks i are considered, with $\mathcal{I}$ as the set of all tasks. For determining the timing of resource interactions during task operation, θ_i defines the time relative to the start of a task i and τ_i defines the total task duration. The integer variable $N_{i,t-\theta}$ and the continuous variable $\xi_{i,t-\theta}$ define the start and extent of operation of task i starting at time t. $\mu_{i,r,\theta}$ and $\nu_{i,r,\theta}$ are known constants which define the interactions with resources during operation, i.e., negative values mean consumption and positive values mean production of a resource. $\mu_{i,r,\theta}$ represents interactions with resources independent of the extent of operation. $\nu_{i,r,\theta}$ defines the amount of resource consumed/produced in relation to the task extent $\xi_{i,t-\theta}$. To account for the addition or removal of resources from the process, $\Pi_{r,t}$ defines external resource flows such as the electricity supply from the grid.

To illustrate the structure and application of the parameters, Fig. 2 shows an exemplary task T1, which interacts with resources A to F. The task T1 starts in time step t_1 ($N_{\mathrm{T1,1}} = 1$) and has an operating duration of 3 time steps ($\tau_{\mathrm{T1}} = 3$). The parameters $\mu_{\mathrm{T1},r,\theta}$ and $\nu_{\mathrm{T1},r,\theta}$ for the interactions with resources A to F are shown with the respective timing that is defined by θ which refers to the delay from the start of the task. For example, resource A is consumed in the first three time steps of the task duration ($\nu_{\mathrm{T1,A,0}}$, $\nu_{\mathrm{T1,A,1}}$, $\nu_{\mathrm{T1,A,2}}$) which represents a continuous material demand during operation. Similarly, resource E is produced continuously during this time ($\nu_{\mathrm{T1,E,0}}$, $\nu_{\mathrm{T1,E,1}}$, $\nu_{\mathrm{T1,E,2}}$), hence representing a continuous production of E. Resources B and F interact with the process just during the beginning and end of the task. Therefore, these resources represent an initial consumption/charge and final production/discharge of materials. Resource C is consumed only once in the middle of the operation ($\nu_{\mathrm{T1,C,1}}$), corresponding to a one-time material demand. Resource D represents an equipment which is consumed/blocked at the beginning ($\mu_{\mathrm{T1,D,0}} = -1$) and produced/released at the end ($\mu_{\mathrm{T1,D,0}} = +1$) of operation, which means that the initial amount of D ($R_{\mathrm{D,0}}$) represents the number of available equipment D.

As this equipment is required for the task operation ($\mu_{\mathrm{T1,D},0} = -1$), the amount limits the instances of task T1 that can operate at the same time.

The amount of a resource r which can be carried over to the next time period is limited by

$$R_{r,t}^{\min} \leq R_{r,t} \leq R_{r,t}^{\max} \quad \forall\, r \in \mathcal{R},\, t \in \mathcal{T}, \tag{4}$$

where $R_{r,t}^{\min}$ and $R_{r,t}^{\max}$ are lower and upper bounds. These bounds basically describe the storage capacity of resources in the process which can be utilized for a more flexible operation.

Further, constraints on the tasks set the operational limits for the magnitude of operation, according to

$$V_i^{\min} N_{i,t} \leq \xi_{i,t} \leq V_i^{\max} N_{i,t} \quad \forall\, i \in \mathcal{I},\, t \in \mathcal{T},\, r \in \mathcal{R}, \tag{5}$$

where $V_i^{\min}$ and $V_i^{\max}$ are the lower and upper operational limits of the respective task.

Based on these equations, tasks can be defined with their respective operating times and material demands. Additional constraints and assumptions specific to the process and our model are explained in the following.

Energy-intensive industries such as copper production typically run continuously. Thus, we want to avoid any additional waiting times of tasks due to empty material inventories. To this end, the initial inventory of resources $R_{r,0}$ needs to be defined so that tasks throughout the process can directly start their operation. To find optimal initial material resource inventories, the initial inventories are defined as variables in the optimization problem. To prevent the generation of resources through $R_{r,0}$, a cyclic constraint is introduced such that inventories at the beginning and at the end of a scheduling horizon must be identical. The cyclic constraint is written as

$$R_{r,0} = R_{r,t_{\max}} \quad \forall\, r \in \mathcal{R}_{cyc}, \tag{6}$$

where $R_{r,0}$ are the initial excess resource levels, $R_{r,t_{\max}}$ the final excess resource levels, and R_{cyc} is the set of resources affected by the cyclic constraint, i.e., all materials with available storage volume $R_{r,t}^{\max}$, excluding the final product. The cyclic constraint also applies to the equipment resources. Therefore, all tasks must be completed at the end of the schedule so that all equipment is available for the beginning of the next schedule.

Converting includes the sub-process of slag-blowing and copper-blowing. These blowing processes generate such large offgas streams that only two of the three converters are allowed to blow simultaneously (Schlesinger et al., 2011). Not being able to operate all converters at once is a typical limitation also mentioned for the plant in Pradenas et al. (2006) and for other plants in Schlesinger et al. (2011). However, the converting task also includes the loading and unloading of the converter. Thus, we assume that the operation of all three converters may overlap as long as no more than two converters are blowing. As this constraint is caused by the offgas system, it is implemented by limiting the equipment of the converter offgas handling system to two by

$$R_{\mathrm{coffh},0} = 2, \tag{7}$$

where $R_{\mathrm{coffh},0}$ is the initial number of converting offgas handling systems. Since the converting offgas handling task requires one instance of this equipment, only two instances can operate at the same time.

Since offgases are always generated during the converter blow, this constraint directly affects the converter scheduling, as we assume that the generated offgases must be treated immediately and cannot be stored. Accordingly, their maximum excess resource level is defined as

$$R_{\mathrm{coffg},t}^{\max} = 0 \quad \forall\, t \in \mathcal{T}, \tag{8}$$

where $R_{\mathrm{coffg},t}^{\max}$ is the upper bound of the excess resource level of the converting offgas. Thus, the offgas handling task must handle the offgas in the time step it is produced so that no excess offgas is left.

The RTN structure of our model is presented in Fig. 3. Tasks include the flash smelting, converting, fire-refining, and respective transport tasks, which do not have significant direct electricity demands but are required to capture the production volume and operating schedule. To limit the model size, further material streams and tasks are only included if they lead to an electricity demand and thus are relevant for the DR potential. Material buffers are introduced where material can accumulate or be stored, e.g., matte is accumulated in the flash furnace bath (Schlesinger et al., 2011) and copper anodes can be stored (Navarra et al., 2016).

As the many molten materials cannot be stored, the model structure needs to represent that the material occupies a vessel until it is transported to the next vessel. The respective structure in our model is explained for the example of the fire refining and the related materials (Fig. 3): The transport task of the blister copper consumes an empty anode furnace and blister copper to produce an anode furnace filled with blister copper. Simultaneously, a converter with blister copper is consumed, and an empty converter is returned. The fire-refining task then processes the material and produces molten copper, occupying the anode furnace until the casting task is finished.

Other materials without a buffer that have to be handled right away are the offgases, compressed air, and oxygen. Storage capacities for oxygen and compressed air are not included in the reference case due to a lack of data. However, we evaluate their influence as part of the sensitivity analysis.

3.3. Parameters and data

Based on the given structure and equations, our scheduling model requires parameters for operating times, operating capacities, resource interactions, electricity demands of all tasks as well as time-varying electricity prices. These parameters are gathered from the literature (Schlesinger et al., 2011; Coursol et al., 2010; Ramachandran et al., 2003) and are used as fixed recipes in the model. Thus, the overall operating times and specific material demands are fixed for each task. An overview of the process tasks and their parameters can be found in the Appendix. The time-varying prices of electricity are based on the hourly electricity prices of the day-ahead market in Germany in 2019 (Bundesnetzagentur SMARD.de, 2020b).

As the electrorefining of copper is the most electricity-intensive task, and therefore often considered as the most promising source of DR potential in copper production (Gils, 2014; Röben et al., 2019), we want to highlight the respective parameters and chosen simplifications in our model.

Producing a copper cathode by electrorefining typically takes 6–8 days. However, a copper anode stays around 21 days in the electrorefining bath, which means that an anode takes part in around three cathode cycles (Schlesinger et al., 2011). Since the copper is plated continuously when a current is applied, we simplify the electrorefining to a continuous task in our model. We assume that this simplification is also justifiable because plants have a large number of electrolytic cells grouped to separate sections, e.g., 1080 cells are mentioned in literature for our example plant (Schlesinger et al., 2011). In result, some sections will be nearly finished during most times. Assuming that 20 cells are part of each section, the number of sections is 54. Assuming further that the average plating takes 7 days, approximately 7.7 sections are completed per day, which is roughly equivalent to one section every 3 h. Thus, we assume that operational flexibility can be achieved by changing operation of individual sections in a plant and that turning off a section does not lead to negative effects on the product. This assumption seems reasonable as the considered plant already participates with it's electrorefining load in DR programs for interruptible loads (NEW 4.0 - Norddeutsche Energiewende, 2019). However, it could still be necessary to keep a minimum current in sections loaded with anodes and cathodes to avoid negative impacts

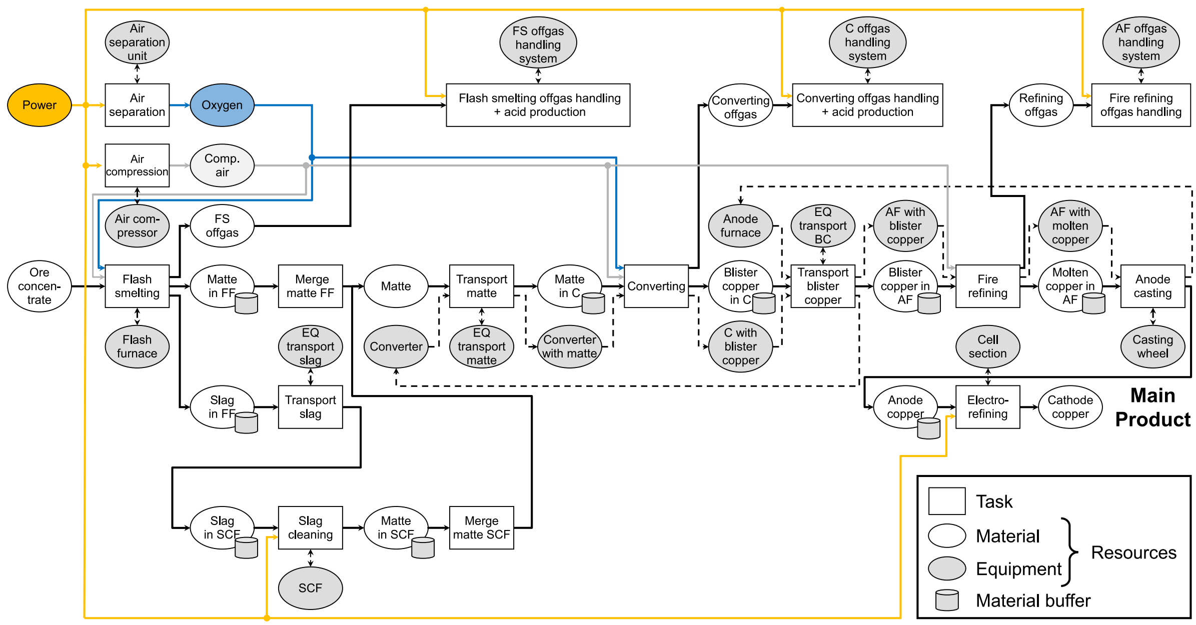

Fig. 3. Resource-task network (RTN) structure of the representative copper-production process. Interactions between tasks (rectangles) and resources (ellipses) require materials (solid line) or equipment (dashed line). The resources include equipment (gray ellipses) and materials (white ellipses). We use the following abbreviations: anode furnace (AF), converter (C), equipment (EQ), flash furnace (FF), flash smelting (FS), and slag-cleaning furnace (SCF). The power (yellow), oxygen (blue), and compressed air (gray) are marked in color to guide the readers eye and make it easier to distinguish between the lines.

on operation. Since we had no data on such a threshold, it was not considered in our analysis but can be easily added to the model.

The peak production of one section is calculated to 0.803 t/h, assuming the stated annual electrorefining capacity of 380,000 t (Schlesinger et al., 2011) and 54 sections operating the whole year (8760 h). As the copper anodes have to be removed from the cell before they become structurally unstable and fall into the cell, an average mass of 11% anode copper remains and is returned to the process as scrap. To represent this incomplete conversion of anode copper to cathode copper, a parameter of $\nu_{erf,ac,0} = -1.124\,\mathrm{t_{ac}/t_{cc}}$ defines the required input per ton of cathode copper in the electrorefining step. The specific electricity demand is $\nu_{erf,el,0} = -350\,\mathrm{kWh/t}$ cathode copper based on the average demand of electrolytic refining (300 to 400 kWh/t) (Schlesinger et al., 2011).

3.4. Analysis approach

To evaluate the economic impact of optimal operation throughout a full year, we use the following procedure.

First, we analyze the influence of the length of the chosen scheduling horizon t_{max} on the maximum production volume by optimizing the production volume under increasing scheduling horizons and evaluate the achieved average hourly production. Based on this analysis, we select a scheduling time horizon for the subsequent optimizations that does not significantly constrain the production volume by being too short, but is also not too long for reasons of computational tractability.

We then split the year into equal time periods based on the determined scheduling time horizon. We determine the maximum production $R^{\mathrm{ref}}_{\mathrm{cc},t_{\mathrm{max}}}$ and starting resource levels $R^{\mathrm{ref}}_{r,0}$ by maximizing the copper production volume neglecting the electricity costs (Eq. (1)). To obtain the identical maximum production ($R^{\mathrm{ref}}_{\mathrm{cc},t_{\mathrm{max}}}$) in the electricity cost minimization (Eq. (2)), we subsequently fix the copper production volume and starting resource levels ($R^{\mathrm{ref}}_{r,0}$) to the results of the reference schedule, i.e.,

$$R_{\mathrm{cc},t_{\mathrm{max}}} = R^{\mathrm{ref}}_{\mathrm{cc},t_{\mathrm{max}}}, \tag{9}$$

$$R_{r,0} = R^{\mathrm{ref}}_{r,0} \quad \forall r \in \mathcal{R}. \tag{10}$$

Due to the cyclic constraint (Eq. (6)), each schedule ends with the same amount of resources as it started with. Since the initial resource levels are identical in each schedule, schedules can be connected to cover longer time-periods such as an entire year.

Besides minimization of electricity costs, we determine the worst-case by maximizing the electricity cost to evaluate the possible electricity cost range for the given maximum production volume. We analyze the results for each schedule with respect to the total electricity cost, task-specific electricity cost, and shifted electricity demand. As the sizing of tasks can significantly impact the available flexibility of a process and hence the DR potential, we also conduct a sensitivity analysis on tasks that appear to limit the production or are power-intensive.

We implement the presented MILP model in Python using the Pyomo package (Hart et al., 2011). The problem is run on a computer with an Intel(R) i7-6700 processor and 32 GB of RAM, using Gurobi 9.0.1 with standard settings and an optimality gap of 1% (Gurobi Optimization, LLC, 2021).

4. Results

In this section, we first analyze the influence of the chosen scheduling horizon on the production volume (Section 4.1). Then, we evaluate the economic results and process operation of the schedules which minimize the electricity costs in comparison to the reference schedule (Section 4.2). Further, task parameters are varied in a sensitivity analysis (Section 4.3) to evaluate the impact on the production volume and electricity cost. Last, we discuss the significance and limitations of our work with regard to the formulated model and discuss possible additions for future work (Section 4.4).

4.1. Influence of scheduling horizon

We analyze the impact of the chosen scheduling time horizon on the achievable average hourly production volume of the representative process (Fig. 4).

As some tasks take a long time to complete, short schedules reduce the averaged hourly production by limiting the amount of batches that can be completed during the scheduling horizon. For example,

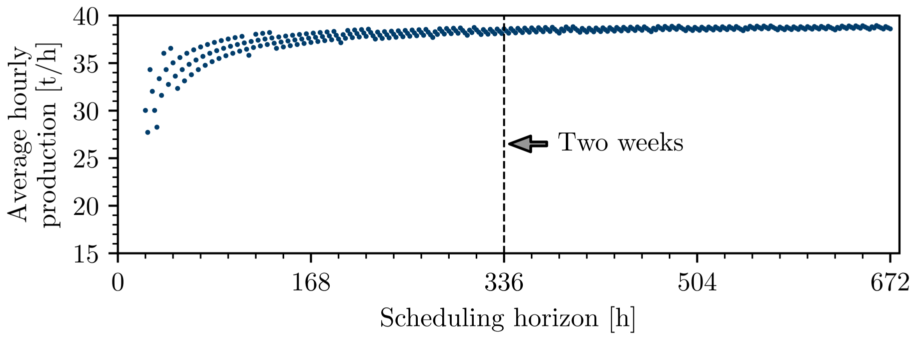

Fig. 4. Influence of the chosen scheduling horizon on the average hourly production of final copper cathodes.

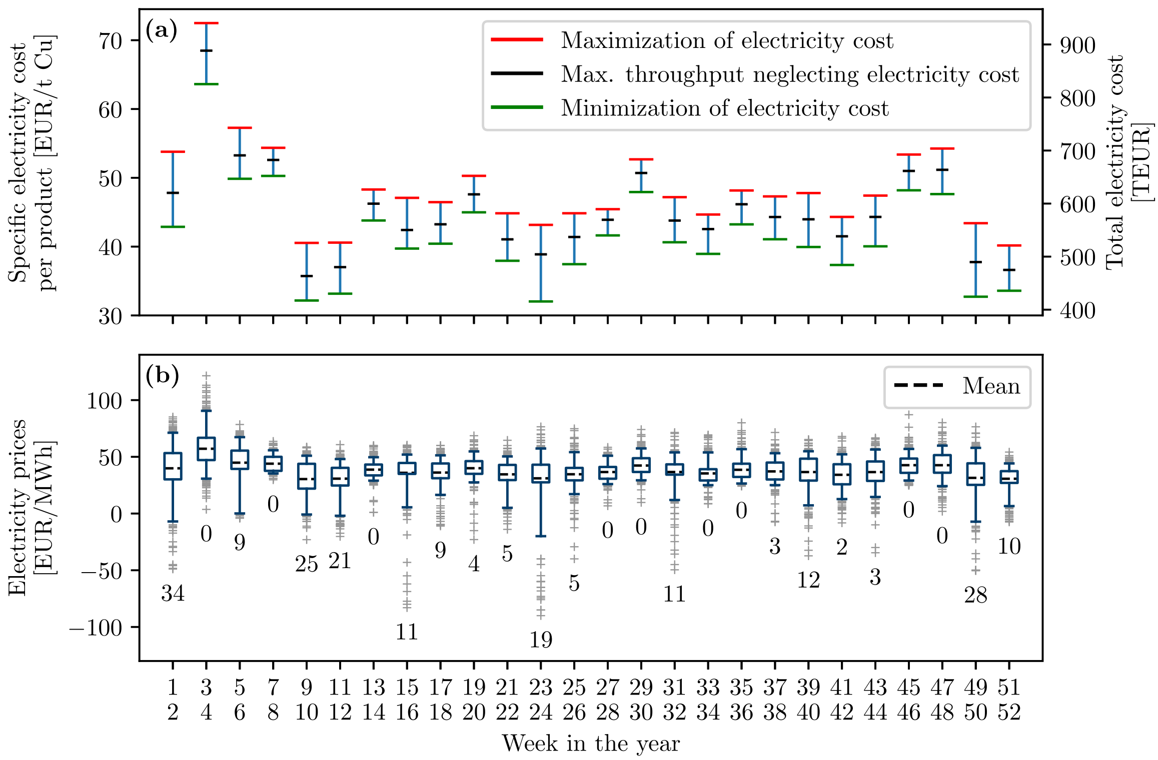

Fig. 5. Overall electricity cost of each two-week schedule (a) for 26 consecutive periods throughout the year and the corresponding electricity prices (b). In (a) the left axis shows the specific electricity costs per ton of copper produced and the right axis the total electricity cost. The maximum throughput optimization (black line) simply neglects the electricity cost. The optimal DR case (green line) minimizes the electricity cost while keeping the final production equal to the maximum throughput case. Electricity cost are maximized (red line) to assess the possible electricity cost range for a given production volume. In (b), the boxplot shows the used day-ahead electricity prices in Germany 2019. The box represents the middle 50% of data points, the whiskers are set to the 5th and 95th percentile, and outliers are marked by plus symbols with the number stating the number of hours with negative prices.

if 4.6 batches could be completed in a scheduling horizon, the optimal schedule can only produce 4 batches as another batch cannot be finished in time. This impact becomes more pronounced for short schedules as a single batch has more relative impact. Being able to finish another batch in time leads to a repeating step-wise structure. Only if the scheduling horizon time increase allows another batch to be finished, the production volume will increase. Thus, the average hourly production drops until this threshold is reached. Notably, the maximum average hourly production quickly approaches a limit, such that further increases of the scheduling horizon offer only minor improvements.

As can be seen from Fig. 4, the production volume is close to the asymptotic limit with a scheduling horizon of two weeks (336 h). We thus select two weeks as scheduling horizon length in all further analyses. The total production in the two-week period $R^{\mathrm{ref}}_{\mathrm{cc},t_{\max}}$ is 12,970 t of cathode copper, which corresponds to an annual copper production of 337,220 t, accounting for 26 schedules in the year. This production volume is close to the value of 340,000 t, which is reported for the main smelter production of the plant our model is based on Mackey and Warner (2019). Note that the total value of 473 kt of cathode copper reported in Aurubis (2019), also takes into account a secondary copper production.

4.2. Cost-optimal schedules

Here, we compare the electricity cost-optimal schedules throughout the year with the reference schedule and determine the DR potential. Further, we analyze the share of each task on the annual electricity costs and the respective cost-reduction potential to evaluate the economic potential of DR in each task.

Fig. 5(a) shows the specific and total electricity costs for each two-week schedule. The optimal scheduling with time-varying electricity prices noticeably decreases the electricity cost per ton of copper produced in all two-week periods, achieving cost reductions from the reference case between 4.4% and 17.6%. Considering all schedules,

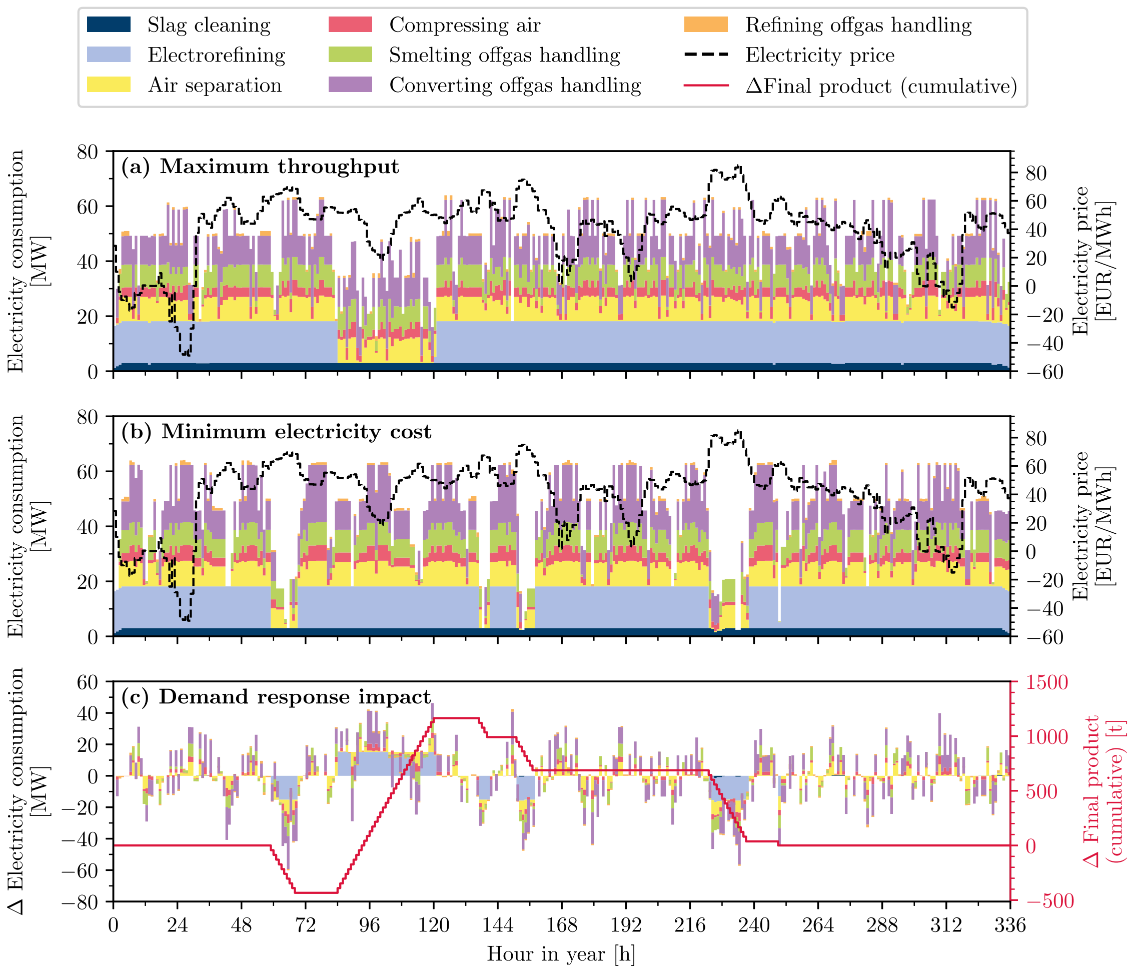

Fig. 6. Electricity consumption of the copper production for the maximum throughput case (a) and the optimal demand response case (b) for identical production volumes under time-varying day-ahead electricity prices shown on the right axis. In (c), the difference between the two cases is shown for electricity consumption and cumulative final production volume. Shown are the first 2 weeks of the year.

the annual electricity cost reduction from the reference case is 7.9%, corresponding to total savings of about 1.2 million Euro.

Since each two-week period has a different electricity price series (Fig. 5(b)), the results show the impact of the electricity prices on the economic result. We observe that both the overall electricity costs and the achievable reduction by optimal scheduling vary significantly. For example, the average electricity prices in the time periods of weeks 49/50 and 51/52 are very similar. However, due to the higher variance in the 49/50 period, the respective costs can be reduced more (13.3% instead of 8.2%), indicating higher economic potential for DR.

The reference case ignored electricity prices. Thus, the resulting electricity costs are arbitrary. To analyze the full range of potential cost savings, we also calculate the worst-case by maximizing the electricity costs for each respective time period (Fig. 5(a)). The corresponding annual cost reduction from the maximum case to the minimum case is 14.2% (2.3 million Euro), which defines the full DR saving potential. Thus, this result shows the overall potential economic range for DR in our model.

To put the specific electricity costs per ton of copper into context, we compare them to the typical revenue streams of a copper production plant. Copper producers generally pay for the copper content in the ore concentrate and recycling materials based on the market price of copper. The actual revenue realized for the treatment and refining of the materials is based on treatment and refining charges (TC/RC) as well as premiums for selling high-purity copper cathodes (Díaz-Borrego et al., 2019). Based on these three revenue streams, we calculate the specific revenue per ton of copper to around 435 EUR/t Cu, applying the charges and premiums in February 2020 (Aurubis, 2020). The specific electricity costs (Fig. 5(a)) indeed constitute a relevant cost factor, as they reach values of 8.2% to 15.7% in relation to the calculated revenue (435 EUR/t Cu) in the reference case. Thus, reducing the electricity costs through DR is economically attractive. Note that the copper price has increased strongly in recent time, which influences the TC/RCs negotiated between mines and smelters. An index of the TC/RCs shows a strong decline due to a high copper demand and limited supply of copper concentrates, which causes smelters to lower their TC/RCs to ensure their ore concentrate supply (Fastmarkets, 2021). Although there are additional revenues, e.g., due to recycling and selling of by-products, lower revenues would further incentivize cost reduction through DR.

Note the negative electricity prices that occur during some hours of the year (Fig. 5(b)). Negative prices result from low demand coinciding with high inflexible generation (Bundesnetzagentur SMARD.de, 2020a). These situations typically occur during times of very high renewable electricity generation, where conventional power plants reduce their generation to their minimum operating point but avoid a complete shutdown for economic reasons (Agora Energiewende, 2020). Continued conventional generation in these times may also be due to combined heat and power generation, regulatory restrictions, or readiness to provide ancillary grid services (Goetz et al., 2014; Bundesnetzagentur SMARD.de, 2020a). To encourage the adoption of renewable electricity generation, market premiums and incentives have often been introduced which can make renewable generation profitable even with negative electricity prices (Bundesnetzagentur SMARD.de, 2020a; Seel

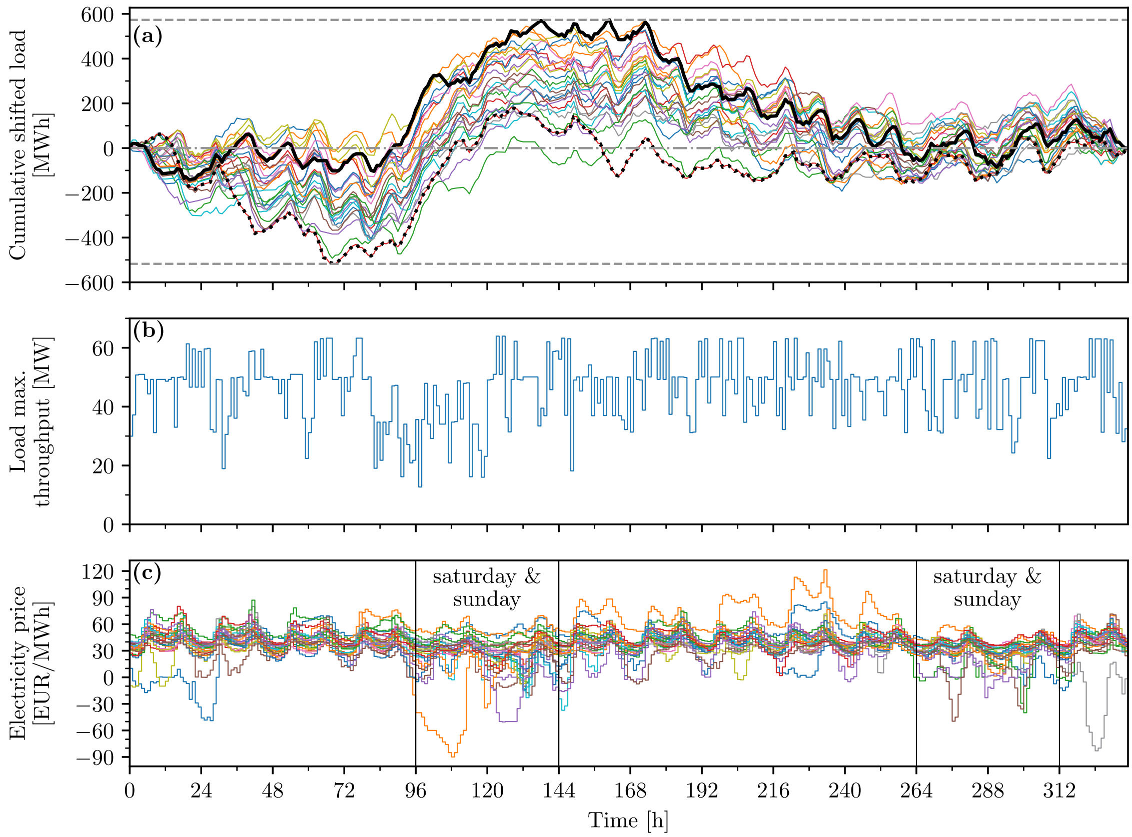

Fig. 7. Cumulative shifted load of each schedule (a), electricity demand of the production volume maximization (b), and the electricity prices (c). The schedules reaching the smallest and largest cumulative load are highlighted by a dotted and solid black line, respectively.

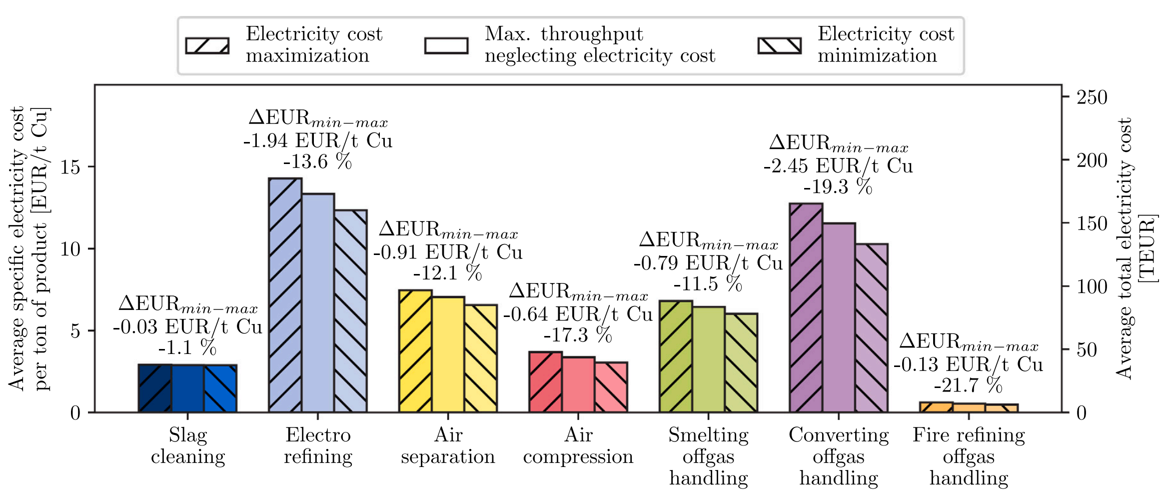

Fig. 8. Task-specific electricity cost averaged over all 26 two-week schedules. The absolute and relative reductions indicate the difference between the maximum and minimum electricity cost.

et al., 2021). Negative electricity prices incentivize restructuring of the energy system, as inflexible generation is affected the most, while storage and flexible operation via DR benefit from negative prices (Winkler et al., 2016).

Fig. 6 compares the electricity demand of the reference case (a) with the minimal electricity cost case (b) for the first two weeks of the year. The schedule with minimized electricity costs shifts production to times with more favorable prices. However, even during negative electricity price hours, not all tasks can operate at full capacity because of dependencies in the plant. The nearly constant operation of the slag-cleaning suggests that this task could be the bottleneck of the production in our representative process (cf. sensitivity analysis in Section 4.3).

The shifted electricity demand is 16.3% (2.53 GWh) in the shown first two weeks, i.e., the overall load increase and decrease from the reference schedule are +2.53 GWh and −2.53 GWh. On average, the shifted load is 2.55 GWh, considering all 26 schedules. The respective annual shifted electricity demand corresponds to 16.5% (66.3 GWh) of the annual electricity demand.

To analyze the impact of optimal DR on process operation, Fig. 6(c) compares the tasks' electricity consumption and the cumulative production volume of cathode copper of the minimum-cost schedule to the reference case. The minimum-cost schedule produces the same amount of cathode copper as the reference case during the first 2.5 days. Still, the minimum-cost schedule allows to provide DR because the intermediate process tasks can shift their operation, as seen by the task-specific electricity demands. The substantial shift in electricity demand illustrates that the process operation strongly responds to the electricity price. Thus, cost-optimal scheduling enables substantial DR potential when considering fluctuating electricity market prices. The final production step, i.e., the electrorefining, can continue operating in the first days due to the intermediate storage of its input material, anode copper. At the end of the schedule, anode copper reaches the same volume due to the cyclical constraints (Eq. (6)). These adjustments in the minimum-cost schedule highlight the potential to utilize the storage capacities in industrial processes for DR. Further, it shows the potential to shift single production steps without impacting the overall production volume.

To further analyze the amount of load shifted over time, we calculate the cumulative load shift for each electricity cost-optimal schedule in comparison to the maximum throughput schedule neglecting the electricity cost (Fig. 7).

The cumulative shifted load of the different schedules (Fig. 7(a)) shows a daily recurring pattern that is also pronounced in the electricity prices (Fig. 7(c)). As we use a schedule of two-week length, each schedule has the same weekly and daily structure, i.e., each schedule starts with a Tuesday and considers the following two weeks. Thus, the typically lower electricity prices at night refer always to the same hours in the scheduling, causing a load increase in electricity-cost-minimized schedules. The strong cumulative shifted load increase starting around hour 84 can be explained by the overall lower electricity demand in the throughput maximization during this time (Fig. 7(b)), which also overlaps with the generally lower electricity prices at Saturday and Sunday (Fig. 7(c)). Therefore, the load in the schedules with minimized electricity costs is generally higher during this time.

The maximum cumulative load shift achieved in one schedule is 573 MWh, which means that the optimal electricity cost schedule consumed 573 MWh of electricity more than the throughput maximization up to this time point. The schedule with the minimum shifted load reaches −517 MWh meaning that the electricity cost schedule consumed 517 MWh less than the throughput maximization up to the respective time point. However, at the end of the two weeks each schedule reaches zero as the load is only shifted in time but not changed in quantity.

We analyze the task-specific electricity costs to evaluate the achievable DR potential per task. Fig. 8 shows the specific electricity costs per ton of copper produced for the individual electricity-consuming tasks averaged over all 26 schedules. The maximum and minimum electricity costs differ most for the converter offgas handling (−2.45 EUR/t Cu (19.3%)), the electrorefining (−1.94 EUR/t Cu (13.6%)), and the air separation (−0.91 EUR/t Cu (12.1%)). Comparing the minimum electricity costs of these tasks to the maximum throughput schedule shows cost reductions of 10.8% for the converter offgas handling, 7.5% for the electrorefining, and 6.9% for the air separation.

While the tasks of smelting, converting, and fire-refining have no direct electricity demand, significant electricity demands are caused by the connected tasks of air separation, air compression, and offgas handling, which are necessary to supply materials required for the operation. The task-specific DR potential shows that scheduling the overall process considering these task dependencies can enable significant DR potential.

4.3. Sensitivity analysis

As discussed in Section 4.2, the slag-cleaning and electrorefining are critical tasks, since the former seems to be the bottleneck and the latter constitutes the task with the largest electricity demand. Thus, we analyze the impact of varying the peak capacity of the slag-cleaning and electrorefining tasks in our model. Further, we determine the additional DR potential from adding storage capacity for compressed air and oxygen.

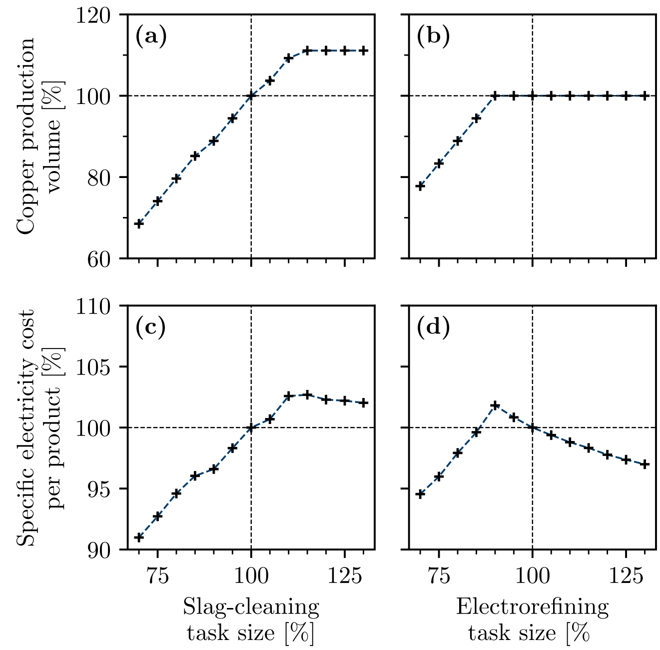

Fig. 9. Impact of the peak capacity of the slag-cleaning and electrorefining on the maximum copper production volume and minimal specific electricity cost. The marked points are the average results of all 26 schedules and the dashed lines are added to guide the reader's eye.

Fig. 9 shows the influence of changing the peak capacity of the slag-cleaning and electrorefining on the production volume and the specific electricity cost per ton of copper, based on the average from all 26 two-week schedules of the year.

Increasing the capacity of the slag-cleaning task increases the overall production volume until it starts to plateau at a capacity of 115% as another task becomes the new bottleneck (Fig. 9(a)). However, the specific electricity costs per ton of copper also slightly increase (Fig. 9(c)) due to the higher production rate increasing the utilization rate of other tasks, which allows for less headroom to shift load. Increasing the capacity beyond 115% decreases the specific electricity cost slightly further as the task can offer more flexibility in operation. Conversely, at decreased capacities, the production volume and the specific electricity costs decline due to the lower utilization rate of other tasks that have more headroom for load shifting available. Thus, the analysis of the bottleneck is of particular importance for the evaluation of the DR potential. The discussion shows that a simple debottlenecking of the process does not necessarily improve the DR potential and cost. In fact, the slag-cleaning is a beneficial bottleneck for DR due to its low electricity demand such that headroom for DR is available for more electricity-intensive tasks.

The electrorefining is analyzed in Fig. 9(b, d). The decrease of the task capacity shows that the electrorefining in our model has available over-capacity since the production volume only decreases at a task capacity below 90%. However, at a capacity of 90%, the specific electricity cost is maximal as the task looses headroom for load shifting (Fig. 9(d)). Similar to the slag-cleaning, once the task becomes the bottleneck, a further decrease of the capacity reduces the specific electricity cost as more headroom is available in the other tasks. An increase in capacity allows for even better utilization of time-varying electricity prices and reduces the electricity cost further, with a 10% capacity increase reducing the total electricity cost by 1.2% (Fig. 9(d)). Again, the analysis shows the complex trade-offs in optimizing copper production and the need for a comprehensive scheduling model.

To create additional flexibility potential, we add storage capacity to the compressed air and oxygen supply (Fig. 10). Due to a lack of data, the storage capacity is based on the number of hours the storage can supply the peak demand of the respective material. The capacities

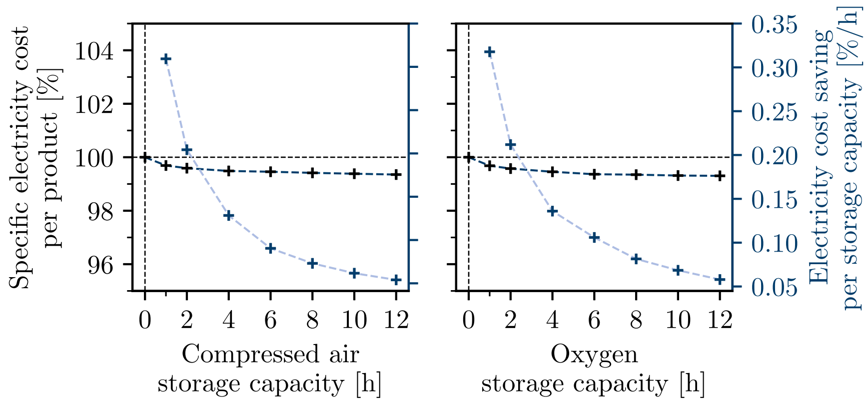

Fig. 10. Impact of adding storing capacity for compressed air and oxygen on the minimal specific electricity cost. The marked points are the average results of all 26 schedules and the dashed lines are added to guide the reader's eye.

of the air compression and air separation are set to the respective peak demand so that the tasks are not arbitrarily over-sized. Thus, the increased DR potential can be accounted to shifting the peak demand of the process and the added storage capacity, allowing for a more flexible process operation. Additional investment costs and potential storage losses are not considered.

The minimal electricity costs decrease when increasing the storage capacities for oxygen and compressed air in relation to the case without the storage capacity. The reason is that the air compression and separation supply time-varying material demands due to the batch operation of other tasks, which means that the peak demands are not required continuously. Thus, depending on the state of operation of these tasks, there is headroom to produce and store oxygen and compressed air, which allows for more DR potential by partially decoupling the supply from the other tasks' operation and enable operation during cheaper electricity prices.

Adding storage capacity for compressed air and oxygen that corresponds to 1 h of peak demand reduces the electricity costs by around 0.3% (Fig. 10). Increasing the storage capacities to 12 h of peak demand reduces the electricity costs only by 0.7% and the specific cost savings of further capacity increases decline strongly. Thus, the first hour of storage capacity brings the largest cost reduction potential (Fig. 10, right axis). This small increase for large storage capacities indicates that a large share of DR potential can already be exploited by the scheduling of the process without this storage capacity. Note that these results lie in the range of the optimality gap of 1%.

4.4. Discussion

The results show substantial potential for demand response in copper production by operating the process in response to time-varying day-ahead market electricity prices. In the following, we discuss the significance and limitations of our results with regard to the underlying model and briefly outline potential future work.

The scarcity of operating data in the public literature may affect the results of our model, as we had to derive the relevant parameters of the process from different literature sources (Ramachandran et al., 2003; Coursol et al., 2010; Schlesinger et al., 2011). As the representative copper production process uses the most common technologies applied, we expect our model to provide a good indication of the DR potential in copper production. Further, the task-specific impacts and sensitivity analysis point to specific areas for DR potential and make the results more applicable. Most importantly, our disclosed model and parameters are easily adaptable to a specific site, enabling readers with access to non-publicly available plant-specific data to replicate and update our analysis.

The parameters from the literature are used as fixed recipes in the model, such that the operating times and specific material demands cannot be adjusted in the scheduling. The reviewed scheduling models for material throughput optimization implement variable operating times for tasks and determine more exact operating times. However, these models typically use continuous-time formulations (cf. Section 3), which makes implementing time-dependent electricity prices and material demands difficult. Further, the respective sources do not fully disclose the chosen parameters, preventing a direct adoption. While our model implements time-dependent electricity prices and material demands and also discloses the used parameters, we see potential in improving the model by using a finer time grid or input-dependent operating times. However, this extension requires more detailed operating data, which we only expect to see in direct collaboration with the industry.

The electricity prices used are all based on hourly day-ahead electricity market prices in Germany in 2019. Importantly, the different two-week time periods show substantial variations in the electricity costs and DR potential (Fig. 5). Thus, the analysis of local electricity prices applicable to a plant is necessary to determine the economic potential for a particular site. Since many copper plants are built near the coast as they receive ore concentrates by ship, we see a further DR potential through the possible proximity to offshore wind power.

Our assessment of the DR potential in copper production by scheduling is the first study to analyze the DR potential of an entire representative copper plant under consideration of dependencies and interactions between the tasks. Our analysis therefore considerably extends beyond existing studies that only consider large electricity consumers, e.g., electric furnaces and electrorefining. The determined DR potential shows that the consideration of tasks without direct electricity demands is required so that connected tasks can operate cost-optimal when supplying materials or treating by-products. Therefore, additional process data can help to further refine the model and improve the representation of the process interactions. Especially, the offgas handling and cleaning systems consume large amounts of electricity, which are required to capture and store the SO_2 by converting it to sulfuric acid. However, such capture systems require capital investment and operating costs, most notably electricity costs. Thus, the local environmental regulations can have a significant impact on the energy-intensity and DR potential of the process.

Our approach of formulating a discrete-time RTN to optimally schedule copper production with DR is consistent with studies in other industries involving batch production. For example, Ave et al. (2019) presented a discrete-time RTN model for steel production that minimizes electricity costs based on the day-ahead and intraday electricity markets, using a non-uniform time grid to reduce computational complexity. Leo et al. (2020) analyzed the DR potential of steel production including uncertain electricity prices formulating a stochastic MILP model based on an RTN formulation. When optimizing continuous production processes, such as air-separation plants (Zhao et al., 2019), studies often consider several operating states and transitions between these states. Some studies even formulate a dynamic optimization problem and integrate the model with the process control as an economic model predictive control (Caspari et al., 2019). Other approaches consider data-driven models to represent the dynamics in the process (Tsay et al., 2019), requiring less computational resources. For future work on copper production scheduling, the inclusion of non-uniform time grids and uncertain electricity prices in a discrete-time RTN seem promising extensions.

5. Conclusions

In this paper, we analyze the demand response (DR) potential of a representative copper production process. To this end, we formulate a mixed-integer linear scheduling model based on the discrete-time Resource-Task Network (RTN) formalism and consider time-varying electricity prices of the Germany day-ahead market.

The optimization of the production schedule based on day-ahead market electricity prices reduces the annual electricity cost by up to 14.2% without reducing the total production volume. Therefore, the scheduling has substantial economic potential, emphasizing the potential for DR in copper production. Although technical limitations are likely to reduce this potential in industrial practice, the shown DR potential is substantial.

The average load shifted is 2.55 GWh in a two-week schedule horizon, based on the electricity cost-optimized 26 schedules throughout the year compared to the reference schedule. Considering all optimized schedules throughout the year, the shifted load amounts to 66.2 GWh (16.5%).

The sensitivity analysis reveals that the slag-cleaning furnace is the bottleneck in our process, limiting the production volume. Expanding the respective peak capacity increases the production volume but slightly reduces the economic DR potential since the rest of the process has less headroom for load shifting. However, the cost-optimal schedule is still able to significantly reduce the costs compared to the reference case.

The electrorefining shows a large DR potential as it is the most electricity-intensive task, reducing its electricity cost by 7.5% on average. Increasing the peak capacity by 10% reduces the overall electricity costs by further 1.2%.

Adding storage capacity to the compressed air and oxygen enables additional operational flexibility due to the fluctuating demand of the batch tasks, even without over-capacity of the corresponding supply tasks. The potential electricity cost reduction could reach up to 0.7% for large storage capacities of oxygen and compressed air. However, 0.3% cost savings would already been achieved by a storage capacity equal to only 1 h of peak demand.

Debottlenecking the process by increasing the slag-cleaning capacity is shown to increase the production volume but also the specific electricity cost per ton of product, since DR flexibility is lost. Thus, optimizing copper production leads to complex trade-offs that require a comprehensive scheduling model.

Further research could focus on the local conditions of specific plant sites such as specific process characteristics, local electricity prices, and environmental regulations. The availability of specific operating data could also improve the model by enabling the use of a finer time grid or input-dependent operating times. Further, specific operating data could allow for the implementation of alternative operating modes. As the reduction of industrial climate change emissions is a critical goal, we see additional flexibility in the decarbonization of the process through Power-to-H_2, which indirectly electrifies fossil-fueled energy demands (Röben et al., 2021).

Nomenclature

Abbreviations

AF	Anode furnace
BC	Blister copper
C	Converter
Comp. air	Compressed air
DES	Discrete-event simulation
DR	Demand response
DSM	Demand side management
EQ	Equipment
FF	Flash furnace
FR	Fire-refining
FS	Flash smelting
MC	Molten anode copper
MILP	Mixed-integer linear program
MT	Matte
OHS	Offgas handling system
RTN	Resource-task network
SCF	Slag-cleaning furnace

Sets

$i \in \mathcal{I}$	Tasks
$r \in \mathcal{R}$	Resources
$t \in \mathcal{T}$	Time steps

Parameters

$\mu_{i,r,\theta}$	Resource interaction in relation to activation of task [-]
$\nu_{i,r,\theta}$	Resource interaction in relation to extent of task [t/t, m^3/t, kWh/t, kWh/m^3]
τ_i	Operating duration of task i [h]
ep_t	Electricity prices in time step t [EUR/kWh]
$R_{r,t}^{\max}$	Maximum resource level [t, m^3, kWh]
$R_{r,t}^{\min}$	Minimum resource level [t, m^3, kWh]
$t_{\max}$	Last time step in $\mathcal{T}$ [-]
$V_i^{\max}$	Maximum task size per batch or hour [t, m^3, kWh]
$V_i^{\min}$	Minimum task size per batch or hour [t, m^3, kWh]

Variables

$\Pi_{r,t}$	External resource streams [t, m^3, kWh]
θ_i	Time relative to the start of task i [h]
$\xi_{i,t}$	Extent of task i in time step t [t, m^3, kWh]
$N_{i,t}$	Start of task i in time step t [-]
$R_{r,t}$	Excess resource level [t, m^3, kWh]

Subscripts

0	Initial
ac	Anode copper
cast	Anode casting
cc	Cathode copper
coffg	Converter offgas
coffh	Converter offgas handling
conv	Converting
cyc	Resources with cyclical constraint
el	Electricity
erf	Electrorefining
fref	Fire refining
fslg	Flash smelting slag
mmff	Merge matte flash furnace
mmscf	Merge matte slag-cleaning furnace
sc	Slag cleaning
tbc	Transport blister copper
tmtt	Transport matte

Table A.1
Task operating limits in alphabetical order.

Task	Unit[a,b]	B_i^{min}	B_i^{max}
Air compression	m^3/h	0	116000
Air separation	m^3/h	0	27500
Anode casting	t/h	67.5	67.5
Converting	t	270	270
Converting offgas handling + acid production	m^3/h	0	155000
Electrorefining[c]	t/h	0	0.803
Fire refining	t	270	270
Fire refining offgas handling	m^3/h	0	101000
Flash smelting[c]	t/h	0	60
Flash smelting offgas handling + acid production	m^3/h	0	68000
Merge matte flash furnace	t	0	450
Merge matte slag-cleaning furnace	t	0	150
Slag cleaning	t	0	66.67
Transport blister copper	t	270	270
Transport matte	t	150	150
Transport slag	t	0	66.67

[a]Volumetric units are stated in relation to standard state.
[b]Units not given in relation to time refer to a batch of the respective task output.
[c]Max. continuous production per section of 20 electrolytic cells based on 380,000 t of annual production (Schlesinger et al., 2011).

Superscripts

max	Maximum
min	Minimum
ref	Reference

CRediT authorship contribution statement

Fritz T.C. Röben: Conceptualization, Methodology, Software, Formal analysis, Validation, Visualization, Writing – original draft. **Diran Liu:** Methodology, Software, Formal analysis, Visualization, Writing – review & editing. **Markus A. Reuter:** Funding acquisition, Writing – review & editing. **Manuel Dahmen:** Conceptualization, Supervision, Writing – review & editing. **André Bardow:** Funding acquisition, Conceptualization, Supervision, Writing – review & editing.

Declaration of competing interest

The authors declare that they have no known competing financial interests or personal relationships that could have appeared to influence the work reported in this paper.

Acknowledgments

The present contribution is supported by the Helmholtz Association under the Joint Initiative 'Energy Systems Integration'.

Appendix. Model parameters

Table A.1 shows the operating limits of all tasks in our model. These parameters refer to one instance of the respective task and are calculated from Schlesinger et al. (2011).

Since the operating time of the batch processes is fixed, we also fix the batch size of each task to the typical parameters mentioned in Schlesinger et al. (2011). The converting batch size is based on the average batch size, which is stated as 260 to 280 t of output material (Schlesinger et al., 2011). The fire-refining is based on the stated batch size of anode copper (Schlesinger et al., 2011).

The casting rate of the anode copper is given as 75 to 80 t/h. Thus, it takes more than three hours to cast the 270 t of anode copper. We round up the casting task to four hours, corresponding to an average casting rate of 67.5 t/h because the minimum time step in our time grid is one hour. The transport tasks are defined so that they can carry a charge of the respective material.

The air separation, air compression, and offgas handling are set to values which do not limit the overall production but which are close to the necessary capacity since we have no process-specific data. As we consider no storage capacity for oxygen and compressed air in the base scheduling model, headroom of the respective tasks has no effect on the

Table A.2
Number of equipment units in the process in alphabetical order.

Equipment	Initial value ($R_{r,0}$)
Air compressor	1
Air separation unit	1
Anode furnace	1
Anode furnace offgas handling system	2
Anode furnace with blister copper	1
Anode furnace with molten copper	0
Casting wheel	1
Cell section (with each 20 electrolytic cells)	54
Converter	1
Converter offgas handling system	2
Converter with matte	1
Converter with blister copper	1
Equipment transport matte	1
Equipment transport slag	1
Equipment transport blister copper	1
Flash furnace	1
Flash furnace offgas handling system	1
SCF virtual equipment	5

Table A.3
Excess resource limits in alphabetical order. Resources with a zero limit have to be directly handled by the following process task.

Resource	Unit	$R_{r,t}^{min}$	$R_{r,t}^{max}$
Anode copper	t	0	∞
Blister copper in converters	t	0	810
Blister copper in anode furnaces	t	0	540
Electricity[a]	kWh	0	0
Cathode copper	t	0	∞
Compressed air	m^3	0	0
Converting offgas	m^3	0	0
Fire-refining offgas	m^3	0	0
Flash smelting offgas	m^3	0	0
Matte	t	0	0
Matte in converters	t	0	450
Matte in flash furnace	t	109	273
Matte in slag-cleaning furnace	t	0	149
Molten anode copper in anode furnace	t	0	540
Ore concentrate[a]	t	0	0
Oxygen	m^3	0	0
Slag in flash furnace	t	126	294
Slag in slag-cleaning furnace	t	429	515

[a]Electricity and ore concentrate are inputs to the process.

Table A.4
Parameters of the continuous tasks for interaction with material $\nu_{i,r,0}$ and equipment $\mu_{i,r,0}$. The required equipment units are returned in the next time step ($\mu_{i,r,1} = 1$).

Task/Resource	Unit[a]	Value	Reference/Comment
Air compression	m^3/h	116000	Task peak capacity
Air compressor	–	−1	Equipment
Electricity	kWh/m^3	−0.05	Based on Coursol et al. (2010)
Compressed air	m^3/m^3	1.0	
Air separation	m^3/h	27500	Task peak capacity
Air separation unit	–	−1	Equipment
Electricity	kWh/m^3	−0.407	Based on Coursol et al. (2010)
Oxygen	m^3/m^3	1.0	
Converting offgas handling	m^3/h	155000	Task peak capacity
Converter OHS[b]	–	−1	Equipment
Electricity	kWh/m^3	−0.0675	Based on Coursol et al. (2010) and Schlesinger et al. (2011)
Converting offgas	m^3/m^3	−1.0	
Electrorefining	t/h	0.803	Task peak capacity
Cell section	–	−1	Equipment
Anode copper	t/t	−1.124	89% utilization of anodes Schlesinger et al. (2011)
Electricity	kWh/t	−350	Mean from Schlesinger et al. (2011)
Cathode copper	t/t	1.0	
Fire refining offgas handling	m^3/h	101000	Task peak capacity
Anode furnace OHS[b]	–	−1	Equipment
Electricity	kWh/m^3	−0.0085	Based on Coursol et al. (2010) and Schlesinger et al. (2011)
Fire-refining offgas	m^3/m^3	−1.0	
Flash smelting	t/h	60	Task peak capacity
Flash furnace	–	−1	Equipment
Ore concentrate	t/t	−2.14	Based on Schlesinger et al. (2011)
Oxygen	m^3/t	−344.28	Based on Schlesinger et al. (2011)
Compressed air	m^3/t	−400.72	Based on Schlesinger et al. (2011)
Flash smelting offgas	m^3/t	976.55	Based on Schlesinger et al. (2011)
Slag in flash furnace	t/t	1.38	Based on Schlesinger et al. (2011)
Matte in flash furnace	t/t	1.0	
Flash smelting offgas handling	m^3/h	68000	Task peak capacity
Flash furnace OHS[b]	–	−1	Equipment
Electricity	kWh/m^3	−0.1413	Based on Coursol et al. (2010) and Schlesinger et al. (2011)
Flash smelting offgas	m^3/m^3	−1.0	

[a]Volumetric units are stated in relation to standard state.
[b]Offgas handling systems are abbreviated as OHS and include the acid production in case of the flash smelting and converting offgases.

Table A.5
Parameters of the converting task based on Schlesinger et al. (2011) and offgas output on Ramachandran et al. (2003).

$\nu_{conv,r,\theta}$	Unit	$\theta = 0$	$\theta = 1$	$\theta = 2$	$\theta = 3$	$\theta = 4$	$\theta = 5$	$\theta = 6$	$\theta = 7$	$\theta = 8$	$\theta = 9$
Matte	t/t	−0.556	0	−0.556	0	0	0	0	0	0	0
Comp. air	m^3/t	0	−155.6	0	−155.6	−166.7	−166.7	−166.7	−166.7	−166.7	0
Oxygen	m^3/t	0	−3.94	0	−3.94	−4.22	−4.22	−4.22	−4.22	−4.22	0
C Offgas	m^3/t	0	574.1	0	574.1	574.1	574.1	574.1	574.1	574.1	0
BC in C	t/t	0	0	0	0	0	0	0	0	0	1
$\mu_{conv,r,\theta}$	–										
C with MT	–	−1	0	0	0	0	0	0	0	0	0
C with BC	–	0	0	0	0	0	0	0	0	0	1

Table A.6
Parameters of the fire-refining task based on Schlesinger et al. (2011) and offgas output on Coursol et al. (2010).

$\nu_{fref,r,\theta}$	Unit	$\theta = 0$	$\theta = 1$	$\theta = 2$	$\theta = 3$	$\theta = 4$	$\theta = 5$
BC in AF	t/t	−1.0	0	0	0	0	0
Comp. air	m^3/t	0	−0.722	0	0	0	0
Fire-refining offgas	m^3/t	0	373.5	373.5	373.5	373.5	0
MC in AF	t/t	0	0	0	0	0	1
$\mu_{fref,r,\theta}$	–						
AF with BC	–	−1	0	0	0	0	0
AF with MC	–	0	0	0	0	0	1

Table A.7
Parameters of the anode casting task calculated from four hours casting time (Schlesinger et al., 2011).

$\nu_{cast,r,\theta}$	Unit	$\theta = 0$	$\theta = 1$	$\theta = 2$	$\theta = 3$	$\theta = 4$
MC in AF	t/t	−1	−1	−1	−1	0
Anode copper	t/t	0	1	1	1	1
$\mu_{cast,r,\theta}$	–					
Casting wheel	–	−1	0	0	0	1
AF with MC	–	−1	0	0	0	0
AF	–	0	0	0	0	1

operation and DR potential. The impact of the corresponding storage capacity is analyzed in Section 4.3. As explained in Section 3.2, the offgas handling of the converting is set to the capacity of one converter blow with two systems available. The transport tasks are set to the respective batch size which assumes that the corresponding material can be moved in one hour.

The residence time of slag in the slag-cleaning furnace is five hours (Schlesinger et al., 2011). To represent the operating structure of the furnace, we introduce a transport task which moves the slag from the flash smelting to the slag-cleaning furnace. While there is only one slag-cleaning furnace, we implement five equipment resources to represent the residence time of five hours while new material can be

Table A.8
Parameters of the slag-cleaning task calculated from Schlesinger et al. (2011).

$\nu_{\mathrm{sc},r,\theta}$	Unit	$\theta = 0$	$\theta = 1$	$\theta = 2$	$\theta = 3$	$\theta = 4$	$\theta = 5$
Slag in SCF	t/t	0	0	0	0	0	−1
Electricity	kWh/t	−9	−9	−9	−9	−9	0
Matte in SCF	t/t	0.00168	0.00168	0.00168	0.00168	0.00168	0
$\mu_{\mathrm{sc},r,\theta}$	–						
SCF virtual equipment	–	−1	0	0	0	0	1

Table A.9
Parameters of the virtual tasks for merging matte from the flash furnace and slag-cleaning furnace. The output of these tasks is the matte that is transported by the following task and allows supplying the converters with matte from both furnaces.

Merge matte flash furnace		
$\nu_{\mathrm{mmff},r,\theta}$	Unit	$\theta = 0$
Matte in flash furnace	t/t	−1
Matte	t/t	1
Merge matte slag-cleaning furnace		
$\nu_{\mathrm{mmscf},r,\theta}$	Unit	$\theta = 0$
Matte in slag-cleaning furnace	t/t	−1
Matte	t/t	1

Table A.10
Parameters of the transport task handling the matte.

$\nu_{\mathrm{tmtt},r,\theta}$	Unit	$\theta = 0$	$\theta = 1$
Matte	t/t	−1	0
Matte in converters	t/t	0	1
$\mu_{\mathrm{tmtt},r,\theta}$	–		
Converter	–	−1	0
Equipment transport matte	–	−1	1
Converter with matte	–	0	1

Table A.11
Parameters of the transport task handling the slag from the flash furnace.

$\nu_{\mathrm{fslg},r,\theta}$	Unit	$\theta = 0$	$\theta = 1$
Slag in flash furnace	t/t	−1	0
Slag in slag-cleaning furnace	t/t	0	1
$\mu_{\mathrm{fslg},r,\theta}$	–		
Equipment transport slag	–	−1	1

Table A.12
Parameters of the transport task handling the blister copper.

$\nu_{\mathrm{tbc},r,\theta}$	Unit	$\theta = 0$	$\theta = 1$
Blister copper in converter	t/t	−1	0
Blister copper in anode furnace	t/t	0	1
$\mu_{\mathrm{tbc},r,\theta}$	–		
Converter with blister copper	–	−1	0
Converter	–	0	1
Equipment transport blister copper	–	−1	1
Anode furnace	–	−1	0
Anode furnace with blister copper	–	0	1

added at any time. Thus, the slag-cleaning task can start in each time step with a corresponding time period of five hours. If started, the slag-cleaning task consumes electricity over five hours and discards the slag after this time. The retrieved matte is accumulated and returned to the primary process chain. To enable use of matte from SCF and FF to start a converter batch, we implement the virtual tasks merge matte FF and merge matte SCF. These tasks are given capacities that do not limit operation.

The matte from the flash furnace is typically charged in the converter in several steps followed by oxidation of the ferrous sulfide (FeS) in the matte (Schlesinger et al., 2011). In the absence of detailed process-specific data, we assume that the matte is charged into the converter in two steps, each followed by one hour of slag blowing (Table A.5), as matte is generally charged step-by-step and the slag blow takes 2 h (Schlesinger et al., 2011).

In Table A.2, we present the number of each equipment available for our reference plant based on Schlesinger et al. (2011). The converter and anode furnaces are assumed to start in different states of operation.

The excess resource limits in Table A.3 are based on average material limits of our reference production process (Schlesinger et al., 2011), e.g., the flash smelting and slag-cleaning furnace material limits are based on the allowed volumes in the furnace multiplied with the average material densities (Schlesinger et al., 2011). The material limits for the materials in the converters and anode furnaces are based on the maximum amount of equipment and material capacity for the respective material, e.g., two anode furnaces with a batch size of 270 t mean an upper bound of blister copper in anode furnaces of 540 t. To prevent unrealistic storing of material, the transport tasks require the respective equipment, thus accounting for a vessel holding the material (cf. Section 3.2) and the corresponding amount of material being transported.

Table A.4 shows the material interactions of the continuous tasks in our model while Tables A.5–A.12 present the material interactions of the batch processes.

References

Agora Energiewende, 2020. Agorameter. https://www.agora-energiewende.de/service/agorameter/chart/power_generation/01.01.2019/31.12.2019/. (Accessed 06 July 2020).

Aurubis, 2019. Environmental Protection in the Aurubis Group. Report, Aurubis AG., https://www.aurubis.com/binaries/content/assets/aurubis-en/dateien/responsibility/environmental-statement/2019_aurubis_ag_environmental_statement_en.pdf. (Accessed 18 December 2019).

Aurubis, 2020. Copper Mail No. 181. Report, Aurubis AG, https://www.aurubis.com/en/investor-relations/news-and-reports/copper-mail/copper-mail-update. (Accessed 16 February 2021).

Ave, G.Dalle., Harjunkoski, I., Engell, S., 2019. A non-uniform grid approach for scheduling considering electricity load tracking and future load prediction. Comput. Chem. Eng. 129, 106506. http://dx.doi.org/10.1016/j.compchemeng.2019.06.031.

Bundesnetzagentur SMARD.de, 2020a. Negative electricity prices. Web page. Bundesnetzagentur. https://www.smard.de/page/en/topic-article/5892/15618. (Accessed 24 March 2022).

Bundesnetzagentur SMARD.de, 2020b. SMARD strommarktdaten. Web page. Bundesnetzagentur. https://www.smard.de/. (Accessed 13 February 2020).

Caspari, A., Offermanns, C., Schäfer, P., Mhamdi, A., Mitsos, A., 2019. A flexible air separation process: 2. optimal operation using economic model predictive control. AIChE J. http://dx.doi.org/10.1002/aic.16721.

Castro, P.M., Harjunkoski, I., Grossmann, I.E., 2019. Discrete and continuous-time formulations for dealing with break periods: Preemptive and non-preemptive scheduling. European J. Oper. Res. 278, 563–577. http://dx.doi.org/10.1016/j.ejor.2019.04.025.

Castro, P.M., Sun, L., Harjunkoski, I., 2013. Resource–Task network formulations for industrial demand side management of a steel plant. Ind. Eng. Chem. Res. 52, 13046–13058. http://dx.doi.org/10.1021/ie401044q.

Coursol, P., Mackey, P.J., Díaz, C., 2010. Energy consumption in copper sulphide smelting. In: Proceedings of Copper 2010. pp. 649–668.

Deetman, S., Pauliuk, S., van Vuuren, D.P., van der Voet, E., Tukker, A., 2018. Scenarios for demand growth of metals in electricity generation technologies, cars, and electronic appliances. Environ. Sci. Technol. 52, 4950–4959. http://dx.doi.org/10.1021/acs.est.7b05549.

Díaz-Borrego, F.J., Miras-Rodríguez, M.d.M., Escobar-Pérez, B., 2019. Looking for accurate forecasting of copper TC/RC benchmark levels. Complexity 2019, 1–16. http://dx.doi.org/10.1155/2019/8523748.

Elshkaki, A., Graedel, T.E., Ciacci, L., Reck, B.K., 2016. Copper demand, supply, and associated energy use to 2050. Glob. Environ. Change 39, 305–315. http://dx.doi.org/10.1016/j.gloenvcha.2016.06.006.

Fastmarkets, 2021. How copper's mine-supply crunch is driving prices to record highs. https://www.fastmarkets.com/article/3989720/how-coppers-mine-supply-crunch-is-driving-prices-to-record-highs. (Accessed 29 June 2021).
Finn, P., Fitzpatrick, C., 2014. Demand side management of industrial electricity consumption: Promoting the use of renewable energy through real-time pricing. Appl. Energy 113, 11–21. http://dx.doi.org/10.1016/j.apenergy.2013.07.003.
Gils, H.C., 2014. Assessment of the theoretical demand response potential in Europe. Energy 67, 1–18. http://dx.doi.org/10.1016/j.energy.2014.02.019.
Goetz, P., Henkel, J., Lenck, T., Lenz, K., 2014. Negative Electricity Prices: Causes and Effect. Report, Agora Energiewende.
Grave, K., Hazrat, M., Dorband, I., Friedrichsen, N., Arens, M., Aydemir, A., Breitschopf, B., Ordonez, J., Angerer, G., 2014. Strompreise Und Stromkosten AusgewäHlter Industrien. Report, Ecofys, Fraunhofer ISI, https://www.isi.fraunhofer.de/content/dam/isi/dokumente/ccx/2014/Industriestrompreise_Stromkosten.pdf.
Gurobi Optimization, LLC, 2021. Gurobi Optimizer Reference Manual. https://www.gurobi.com.
Harjunkoski, I., Borchers, H.W., Fahl, M., 2006. Simultaneous scheduling and optimization of a copper plant. In: Computer Aided Chemical Engineering 21, 16th European Symposium on Computer Aided Process Engineering and 9th International Symposium on Process Systems Engineering. pp. 1197–1202. http://dx.doi.org/10.1016/S1570-7946(06)80209-9.
Harjunkoski, I., Maravelias, C.T., Bongers, P., Castro, P.M., Engell, S., Grossmann, I.E., Hooker, J., Méndez, C., Sand, G., Wassick, J., 2014. Scope for industrial applications of production scheduling models and solution methods. Comput. Chem. Eng. 62, 161–193. http://dx.doi.org/10.1016/j.compchemeng.2013.12.001.
Hart, W.E., Watson, J.P., Woodruff, D.L., 2011. Pyomo: modeling and solving mathematical programs in python. Math. Program. Comput. 3, 219–260. http://dx.doi.org/10.1007/s12532-011-0026-8.
Heffron, R., Körner, M.F., Wagner, J., Weibelzahl, M., Fridgen, G., 2020. Industrial demand-side flexibility: A key element of a just energy transition and industrial development. Appl. Energy 269, 115026. http://dx.doi.org/10.1016/j.apenergy.2020.115026.
Henckens, M.L.C.M., Worrell, E., 2020. Reviewing the availability of copper and nickel for future generations, the balance between production growth, sustainability and recycling rates. J. Clean. Prod. 264, 121460. http://dx.doi.org/10.1016/j.jclepro.2020.121460.
IEA, 2021. The Role of Critical Minerals in Clean Energy Transitions. Report, IEA (International Energy Agency, https://www.iea.org/reports/the-role-of-critical-minerals-in-clean-energy-transitions.
Korpi, M., Suominen, O., Jansson, J., Pihlasalo, J., Vilkko, M., 2019. Plant-wide optimization of a copper smelter: how to do it in practice? In: Proceedings of the 10th European Metallurgical Conference, EMC 2019, GDMB. pp. 95–106, https://trepo.tuni.fi/handle/10024/122137.
Kuipers, K.J.J., van Oers, L.F.C.M., Verboon, M., van der Voet, E., 2018. Assessing environmental implications associated with global copper demand and supply scenarios from 2010 to 2050. Global Environ. Change 49, 106–115. http://dx.doi.org/10.1016/j.gloenvcha.2018.02.008.
Leo, E., Dalle Ave, G., Harjunkoski, I., Engell, S., 2020. Stochastic short-term integrated electricity procurement and production scheduling for a large consumer. Comput. Chem. Eng. 107191. http://dx.doi.org/10.1016/j.compchemeng.2020.107191.
Mackey, P.J., Warner, A.E.M., 2019. Around the copper world in eighty days a virtual tour of world copper operations and technologies. In: 58th Annual Conference of Metallurgists (COM) Hosting the 10th International Copper Conference 2019.
Merkert, L., Harjunkoski, I., Isaksson, A., Säynevirta, S., Saarela, A., Sand, G., 2015. Scheduling and energy – Industrial challenges and opportunities. Comput. Chem. Eng. 72, 183–198. http://dx.doi.org/10.1016/j.compchemeng.2014.05.024.
Moreno-Leiva, S., Haas, J., Junne, T., Valencia, F., Godin, H., Kracht, W., Nowak, W., Eltrop, L., 2019. Renewable energy in copper production: A review on systems design and methodological approaches. J. Cleaner Prod. 118978. http://dx.doi.org/10.1016/j.jclepro.2019.118978.
Navarra, A., 2016. Automated scheduling and scientific management of copper smelters. Miner. Process. Extr. Metall. 125, 39–44. http://dx.doi.org/10.1179/1743285515Y.0000000018.
Navarra, A., Kuan, S.H., Parra, R., Davis, B., Mucciardi, F., 2016. Debottlenecking of conventional copper smelters. In: Proceedings of the 2016 International Conference on Industrial Engineering and Operations Management, Kuala Lumpur, Malaysia, 8-10 2016.
Navarra, A., Marambio, H., Oyarzun, F., Parra, R., Mucciardi, F., 2017. System dynamics and discrete event simulation of copper smelters. Miner. Metall. Process. 34, 96–106. http://dx.doi.org/10.19150/mmp.7510.
NEW 4.0 - Norddeutsche Energiewende, 2019. Erfolgsfaktoren der integrierten Energiewende (Annex). Report, Schaufenster intelligente Energie (SINTEG), Bundesministeriums für Wirtschaft und Energie (BMWi, https://www.new4-0.de/ergebnisse/. (Accessed 29 June 2021).
Pantelides, C.C., 1994. Unified frameworks for optimal process planning and scheduling. In: Proceedings on the Second Conference on Foundations of Computer Aided Operations. Cache Publications New York, pp. 253–274.
Papadaskalopoulos, D., Moreira, R., Strbac, G., Pudjianto, D., Djapic, P., Teng, F., Papapetrou, M., 2018. Quantifying the potential economic benefits of flexible industrial demand in the european power system. IEEE Trans. Ind. Inf. 14, 5123–5132. http://dx.doi.org/10.1109/tii.2018.2811734.
Paulus, M., Borggrefe, F., 2011. The potential of demand-side management in energy-intensive industries for electricity markets in Germany. Appl. Energy 88, 432–441. http://dx.doi.org/10.1016/j.apenergy.2010.03.017.
Pradenas, L., Campos, A., Saldaña, J., Parada, V., 2011. Scheduling copper refining and casting operations by means of heuristics for the flexible flow shop problem. Pesqui. Oper. 31, 443–457. http://dx.doi.org/10.1590/s0101-74382011000300002.
Pradenas, L., Zúñiga, J., Parada, V., 2006. CODELCO chile programs its copper-smelting operations. INFORMS J. Appl. Anal. 36, 296–301. http://dx.doi.org/10.1287/inte.1060.0207.
Ramachandran, V., Díaz, C., Eltringham, T., Lehner, T., Mackey, P.J., Newman, C.J., Tarasov, A., 2003. In: Díaz, C., Kapusta, J., Newman, C. (Eds.), Primary Copper Production - a Survey of Operating World Copper Smelters. Copper, 2003.
Röben, F.T.C., Bau, U., Dahmen, M., Reuter, M.A., Bardow, A., 2019. Demand side management potential of primary copper production. In: Stanek, W., Gładysz, P., Werle, S., Adamczyk, W. (Eds.), Proceedings of ECOS 2019 - the 32nd International Conference on Efficiency, Cost, Optimization, Simulation and Environmental Impact of Energy Systems. Institute of Thermal Technology, Silesian University of Technology, pp. 1619–1629.
Röben, F.T.C., Schöne, N., Bau, U., Reuter, M.A., Dahmen, M., Bardow, A., 2021. Decarbonizing copper production by power-to-hydrogen: A techno-economic analysis. J. Clean. Prod. 306, 127191. http://dx.doi.org/10.1016/j.jclepro.2021.127191.
Schipper, B.W., Lin, H.C., Meloni, M.A., Wansleeben, K., Heijungs, R., van der Voet, E., 2018. Estimating global copper demand until 2100 with regression and stock dynamics. Resour. Conserv. Recycling 132, 28–36. http://dx.doi.org/10.1016/j.resconrec.2018.01.004.
Schlesinger, M.E., King, M.J., Sole, K.C., Davenport, W.G., 2011. Extractive Metallurgy of Copper, Fifth ed. Elsevier, http://dx.doi.org/10.1016/C2010-0-64841-3.
Seel, J., Millstein, D., Mills, A., Bolinger, M., Wiser, R., 2021. Plentiful electricity turns wholesale prices negative. Adv. Appl. Energy 4, 100073. http://dx.doi.org/10.1016/j.adapen.2021.100073.
Siemon, M., Schiffer, M., Mitra, S., Walther, G., 2020. Value-based production planning in non-ferrous metal industries: Application in the copper industry. IISE Trans. 1–18. http://dx.doi.org/10.1080/24725854.2020.1711992.
Siemon, M., Schiffer, M., Walther, G., 2021. Integrated purchasing and production planning for a non-ferrous metal production network. Omega 98, 102136. http://dx.doi.org/10.1016/j.omega.2019.102136.
Sundaramoorthy, A., Maravelias, C.T., 2011. Computational study of network-based mixed-integer programming approaches for chemical production scheduling. Ind. Eng. Chem. Res. 50, 5023–5040. http://dx.doi.org/10.1021/ie101419z.
Suominen, O., Mörsky, V., Ritala, R., Vilkko, M., 2016. Framework for optimization and scheduling of a copper production plant. In: Kravanja, Z., Bogataj, M. (Eds.), Proceedings of the 26th European Symposium on Computer Aided Process Engineering - ESCAPE 26. Elsevier, pp. 1243–1248. http://dx.doi.org/10.1016/B978-0-444-63428-3.50212-5.
Tsay, C., Kumar, A., Flores-Cerrillo, J., Baldea, M., 2019. Optimal demand response scheduling of an industrial air separation unit using data-driven dynamic models. Comput. Chem. Eng. http://dx.doi.org/10.1016/j.compchemeng.2019.03.022.
Wang, S., Davenport, W., Yao, S., Walters, G., Gonzales, T., Siegmund, A., George, D.B., 2019. Copper smelting: 2019 world copper smelter data. In: Proceedings of the 58th Annual Conference of Metallurgists (COM) Hosting the 10th International Copper Conference 2019, Vancouver, Canada, 18-21 2019.
Wassick, J.M., Ferrio, J., 2011. Extending the resource task network for industrial applications. Comput. Chem. Eng. 35, 2124–2140. http://dx.doi.org/10.1016/j.compchemeng.2011.01.010.
Winkler, J., Gaio, A., Pfluger, B., Ragwitz, M., 2016. Impact of renewables on electricity markets – DO support schemes matter?. Energy Policy 93, 157–167. http://dx.doi.org/10.1016/j.enpol.2016.02.049.
Zhang, Q., Grossmann, I.E., 2016. Enterprise-wide optimization for industrial demand side management: Fundamentals, advances, and perspectives. Chem. Eng. Res. Des. 116, 114–131. http://dx.doi.org/10.1016/j.cherd.2016.10.006.
Zhao, S., Ochoa, M.P., Tang, L., Lotero, I., Gopalakrishnan, A., Grossmann, I.E., 2019. Novel formulation for optimal schedule with demand side management in multiproduct air separation processes. Ind. Eng. Chem. Res. 58, 3104–3117. http://dx.doi.org/10.1021/acs.iecr.8b04964.